

A FLARE EVENT ON THE LONG-PERIOD RS CANUM VENATICORUM SYSTEM IM PEGASI

DEREK L. BUZASI, LAWRENCE W. RAMSEY, AND DAVID P. HUENEMOERDER

Department of Astronomy, The Pennsylvania State University

Received 1986 December 22; accepted 1987 April 28

ABSTRACT

During a monitoring program of the visible and ultraviolet spectra of the long-period RS CVn system IM Pegasi a flare event was detected in the short-wavelength region with *IUE*. This low-resolution spectrum showed enhancements of up to a factor of 5 in some emission lines. Visible spectra obtained some hours earlier failed to show any indication of this event. All of the ultraviolet emission lines normally visible were enhanced significantly more than the normal 30% rotational modulation which is apparently due to the distribution of active regions on the primary star in this system. Emission fluxes of both the quiescent and flare event were used to construct models of the density and temperature variation with height. These models reveal a downward shift of the transition region during the flare. Scaled models of the quiet and flaring solar outer atmosphere are used to estimate the filling factor of the flare event on IM Pegasi at about 30% of the stellar surface. We also note that the pattern of line enhancements of the IM Peg flare is the same as a similar event in λ Andromeda observed previously. This pattern for these long-period systems is, however, distinctly different than that observed in the short-period systems UX Arietis and HR 1099.

Subject headings: stars: binaries — stars: flare — stars: individual (IM Peg) — ultraviolet: spectra
ultraviolet: spectra

I. INTRODUCTION

Although RS CVn systems have been studied extensively in the past decade, observations of flare events from these systems have been very rare. Visual detection of flares on late-type stars is complicated by the low contrast between the flare and the photosphere. In spite of this difficulty, H α and Ca II H and K emission-line flaring has been detected on some systems of this type (see, e.g., Weiler *et al.* 1978; Baliunas *et al.* 1981). Ultraviolet flares have been detected using the *IUE* satellite on UX Ari (Simon, Linsky, and Schiffer 1980) and λ And (Baliunas, Guinan, and Dupree 1984), among others. These observations reveal a preferential enhancement of the transition lines relative to the chromospheric lines similar to that seen in solar flares (Baliunas, Guinan, and Dupree 1984; Linsky 1984). The physical sizes, or filling factors, of these flares are, for the most part, unknown. Linsky (1984) adopts a filling factor of 0.06 for an active region on II Peg, while a large solar flare may reach a covering factor of only 0.001 (Allen 1973).

We observed a large flare event on the long-period RS CVn binary IM Peg. The spectral type of the visible star in this system is K1 III-IV. The star has a spectroscopic orbit of 24.65 days and a rotation period of 24.4 days; it is thus nearly a synchronous system. The distance to the system is estimated to be 200 pc (Eker 1984), while application of the Barnes and Evans relations (Barnes and Evans 1976; Barnes, Evans, and Parsons 1976) yields a radius of $29 R_{\odot}$. The surface gravity was assumed to be $\log(g) = 1.5$, based on an estimated mass of $1 M_{\odot}$.

The observed ultraviolet emission lines lead to a mean emission measure distribution for IM Peg, from which approximate models of the chromosphere and the transition region may be constructed for both the quiescent and for the flaring star. The observed similarities between the flare observed on IM Peg and typical solar flares are sufficient to allow comparison of these models to similar models of solar active regions and

hence a rough determination of the surface covering factor of the flare.

II. OBSERVATIONS AND DATA REDUCTION

During the summers of 1985 and 1986 a total of 10 *IUE* spectra of IM Peg were obtained. All were low-dispersion SWP spectra, with exposure times ranging from 20 to 120 minutes. Pertinent information is summarized in Table 1. Image SWP 26349, a 65 minute exposure obtained on 1985 July 5, was a flare episode. Observed variation between quiescent spectra was apparent and correlated with the phase of the star. However, the degree of rotational modulation thus observed was $\sim 30\%$, while the modulation caused by the flare was over an order of magnitude greater.

The *IUE* data were processed at the Pennsylvania State University using the BMO/FORTH software package, which was entirely adequate to determine the line fluxes.

The low-resolution, quiescent ultraviolet spectrum of IM Peg is shown in Figure 1. It displays emission lines formed in a wide range of excitation conditions, ranging from 6300 K (O I) to 2×10^5 K (N V). Prominent lines are as identified in Baliunas, Guinan, and Dupree (1984), and include N V, O I, C II, Si IV, C IV, He II, C I, Si II, and Si III. The prominent Ly α feature is contaminated by geocoronal emission and is not analyzed. The continuum spectrum is observed to be very flat across the ultraviolet wavelengths.

Figure 2 shows the spectrum of IM Peg observed during the flare episode. In addition to the expected line enhancements, we see that the continuum spectrum is also enhanced, particularly toward the longer wavelengths. Relative line enhancements and other line data are given in Table 2. As in the λ And flare observed by Baliunas, Guinan, and Dupree (1984) on 1982 November 2, peak enhancement occurs in the C IV and N V lines. In addition, it is clear that the transition region lines C II, Si III, Si IV, and C IV are more strongly enhanced, by a

TABLE 1
SUMMARY OF SPECTRA OBTAINED

Date	Image No.	Resolution	Exposure time
1985 Jul 2	SWP 26334	Low	50
1985 Jul 5	SWP 26349	Low	65
1985 Jul 12	SWP 26403	Low	25
1985 Jul 16	SWP 26423	Low	50
1985 Jul 20	SWP 26449	Low	20
1985 Jul 31	SWP 26507	Low	50
1985 Aug 6	SWP 26562	Low	30
1985 Aug 11	SWP 26589	Low	60
1986 May 29	SWP 28400	Low	120
1986 May 29	SWP 28403	Low	65

factor of 2 or more, than the chromospheric lines. This effect is identical to that seen in other ultraviolet stellar flares (see Baliunas, Guinan, and Dupree 1984) and strongly resembles that seen in large solar flares.

Optical spectra obtained at Black Moshannon Observatory hours earlier failed to show any evidence of a flare. Such evidence was also lacking in optical spectra obtained on July 8. Excluding the Ly α geocoronal line, total radiative output from ultraviolet emission lines is about 6×10^{31} ergs s $^{-1}$, so the minimum total radiative output of the flare in the ultraviolet is 2×10^{35} ergs, comparable to that seen in the λ And event. In comparison, the large solar flare of 1973 September 7 lasted about 2 hr and radiated $\sim 10^{31}$ ergs in the ultraviolet portion of the spectrum.

III. EMISSION MEASURE ANALYSIS

The tools of emission measure analysis are briefly outlined here; a more complete discussion can be found in Withbroe (1975) or Jordan and Wilson (1971). Previous applications of

TABLE 2
FLARE EMISSION ENHANCEMENTS IN THE ULTRAVIOLET

FEATURE	λ (Å)	FLUX AT EARTH ($\times 10^{-13}$ ergs cm $^{-2}$ s $^{-1}$)		
		Quiescent	Flare	ENHANCEMENT
N v	1237	9.3	19.0	2.0
O I	1300	16.6	31.6	1.9
C II	1335	9.0	30.3	3.4
Si IV	1392	8.0	30.0	3.8
C IV	1550	14.4	75.6	5.3
He II	1640	6.7	27.2	4.1
C I	1657	7.6	14.4	1.9
Si II	1810	14.7	21.6	1.5
Si III	1892	4.4	15.3	3.5

the technique to stellar chromospheres and coronae include Brown and Jordan (1981), Brown, Ferraz, and Jordan (1984), and Brown *et al.* (1984).

The total surface flux in a collisionally excited, effectively thin emission line can be written as

$$F_k = \frac{6.8 \times 10^{-22}}{\lambda} \frac{\Omega_{12}}{\omega_1} \frac{N_E}{N_H} \int_{\Delta h} g(T) N_e^2 dh. \quad (1)$$

Here Ω_{12} is the collision strength, ω_1 is the statistical weight of the lower level, and N_E/N_H is the element abundance, taken to be solar. The explicitly temperature-dependent quantities are contained in the function $g(T)$:

$$g(T) = T_e^{-1/2} \frac{N_i}{N_e} \exp\left(-\frac{W_{12}}{kT_e}\right), \quad (2)$$

where N_i/N_e is the level population and W_{12} is the excitation energy. Since $g(T)$ is a sharply peaked function of T , following

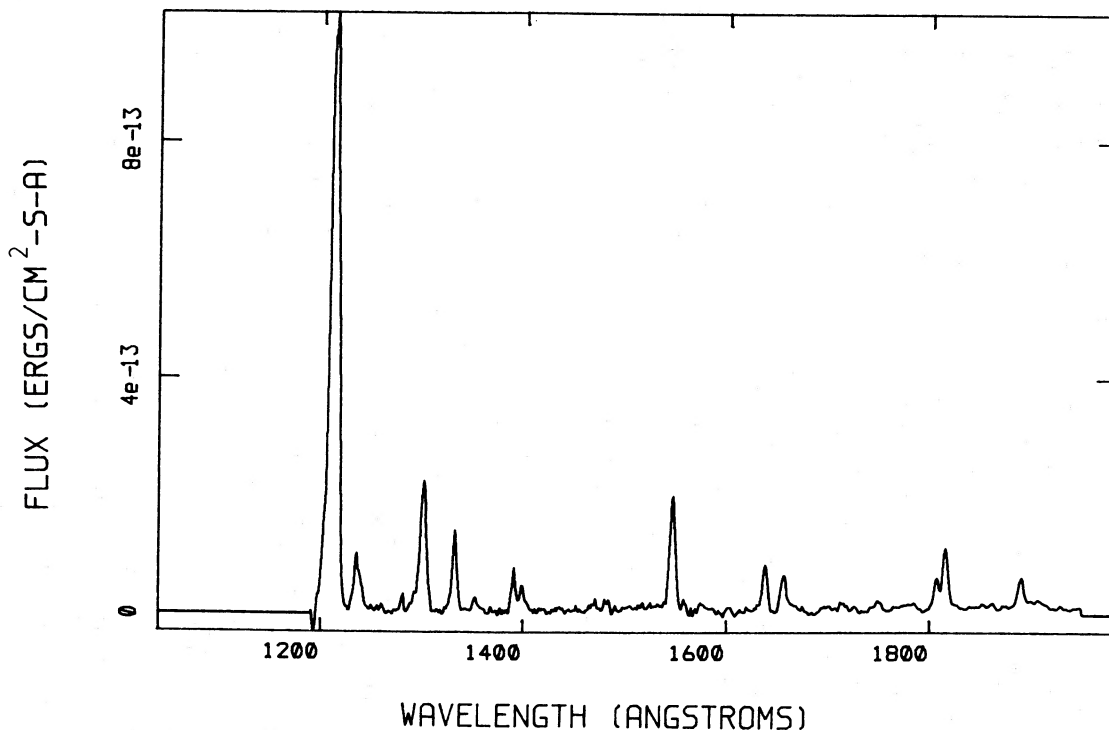


FIG. 1.—Flux observed at Earth from IM Peg during a quiescent period (SWP 28400). Ly α is saturated.

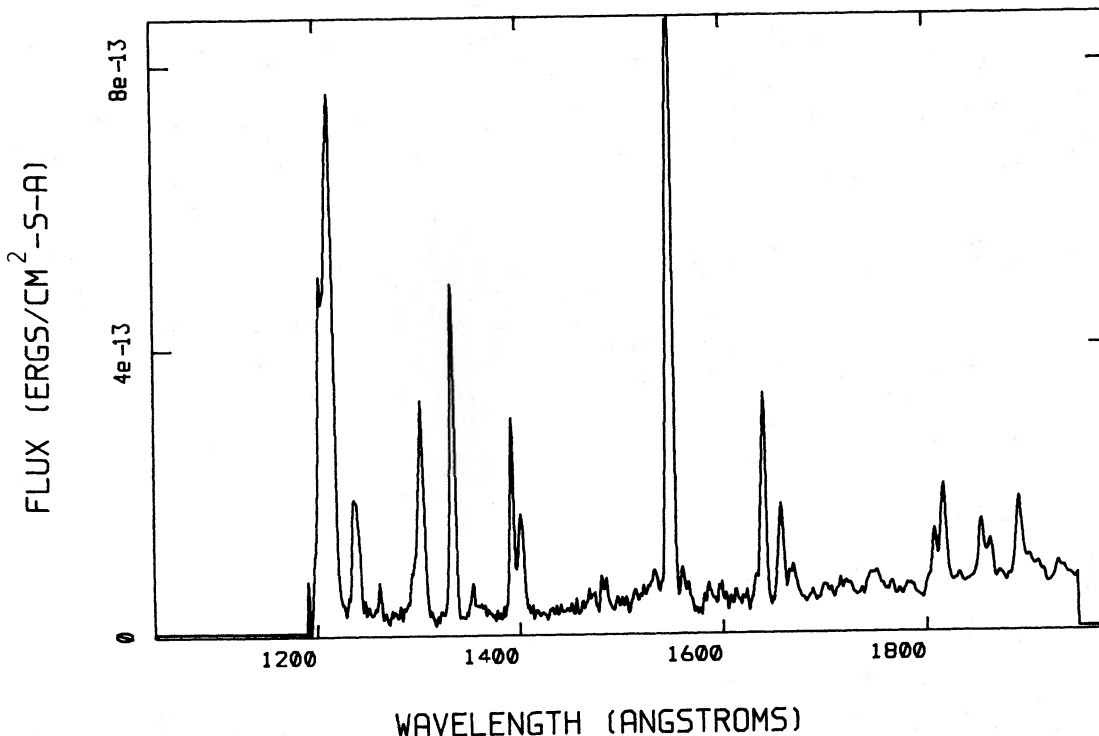


FIG. 2.—Flux observed at Earth from IM Peg during the flare of 1985 July 5 (SWP 26349). Ly α and C IV are saturated.

Brown and Jordan (1981) we can write

$$\int_{T_1}^{T_2} g(T) d \log T = Gg(T_m) \quad (3)$$

over some $\log T = \pm 0.15$ dex, where G is a normalization constant, which may easily be calculated. Thus $g(T)$ can be removed from inside the integral and replaced by $Gg(T)$, where T is the value of T where $g(T)$ is a maximum. This done, we may define the emission measure as

$$EM = \int_{\Delta h} N_e^2 dh. \quad (4)$$

The above discussion assumes that hydrogen is completely ionized, as is the case at $T > 2 \times 10^4$ K, and hence that $N_H = 0.8N_e$. For $T < 2 \times 10^4$ K, this is not the case, and we should write

$$EM = \int_{\Delta h} N_e N_H dh. \quad (5)$$

This formulation applies in our case only to the O I line and requires the use of a model atmosphere, which is unavailable for IM Peg. However, if the part of the atmosphere which is of

interest is restricted to the transition region, we may ignore the O I line and so avoid this problem.

In general, the atomic data adopted are taken from Brown and Jordan (1981) with the exception of the Si IV line, for which data came from Brown *et al.* (1984). Ionization equilibrium data were taken from Jordan (1969). The atomic data used, and the emission measures derived from both the quiescent and flaring IM Peg, are summarized in Table 3.

IV. MODELS OF THE STRUCTURE

The emission measure distribution determined above can be used to calculate spherically symmetric models of the upper chromosphere and transition region. The method outlined below is described in more detail in Jordan and Wilson (1971) and Brown and Jordan (1981).

If we assume that (a) $P_e = N_e T_e$ is constant over Δh , the line formation region, and that (b) $d \log T_e/dh$ is similarly constant, we can write equation (4) as

$$EM = \left| \frac{dh}{d \log T_e} \right|_{\Delta T} \frac{|P_e^2|}{T_m^2} \Delta T d \log T_e \quad (6)$$

TABLE 3
ATOMIC DATA USED AND RESULTING EMISSION MEASURES

Ion	λ (Å)	Ω	ω	N_e/N_H	$\log T_m$	EM (quiescent)	EM (flare)
N V	1237	7.2	2	7.9(-5)	5.3	8.8(28)	1.8(29)
C II	1335	4.2	4	2.5(-4)	4.65	4.2(28)	1.4(29)
Si IV	1392	16.4	2	4.0(-5)	4.9	2.5(28)	9.5(28)
C IV	1550	11.2	2	2.5(-4)	5.0	8.7(27)	4.6(28)
Si II	1810	0.73	4	4.0(-5)	4.5	1.4(30)	2.3(30)
Si III	1892	3.2	1	4.0(-5)	4.8	1.5(28)	5.8(28)

following Jordan and Wilson (1971), or that

$$\frac{dT_e}{dh} = \frac{P_e^2}{1.4 \text{ EM } T_e} \quad (7)$$

If, in addition, we assume (c) hydrostatic equilibrium,

$$\frac{dP_e}{dh} = -7.14 \times 10^{-9} \frac{P_e g_\star}{T_e} \quad (8)$$

the two differential equations may be simultaneously solved to yield a model. A polynomial fit may be adopted to obtain the rule of EM values required for the modeling process.

A starting value of (N_e, T_e) is also needed. Such a starting point may be obtained by assuming that the highest line observed is formed in an isothermal region over one scale height. Then

$$\text{EM} \approx N_e^2 H \quad (9)$$

where

$$H = \frac{kT_e}{\mu m_H g_\star} \quad (10)$$

Thus

$$P_e(\text{min}) = \left(\frac{\text{EM } T_e^2}{H} \right)^{1/2} \quad (11)$$

Using the N v line in the quiescent spectrum gives $P_e(\text{min}) = 8.7 \times 10^{13}$. The resulting model is not exceedingly sensitive to the exact value of $P_e(\text{min})$ used; several models were calculated with different values of $P_e(\text{min})$ at $\log T = 5.3$ and a value of $P_e(\text{min}) = 1.4 \times 10^{14}$ was determined to be appropriate.

A model of IM Peg may similarly be calculated during the flare. If the assumptions is made that the flare is a relatively small atmospheric perturbation, the same top pressure may be used for this model as was used for the quiescent model. The resulting models are summarized in Table 4 and Figure 3. The height scale in Figure 3 is in units of scale heights at $\log T = 4.5$ and has a zero point arbitrarily set at $\log T = 5.4$.

Following Withbroe (1975), we can write

$$\frac{dT}{dh} \sim \frac{P_e^2}{T^2} \frac{1}{Q(T)}, \quad (12)$$

where $Q(T)$ is a differential emission measure defined as

$$Q(T)dT = N_e^2 dh. \quad (13)$$

Then, observing that the differential emission measure in the transition region is approximately constant, we may write

$$h(T) \sim T^3 \quad (14)$$

in the transition region. Thus, we expect steep temperature gradients in the transition region, and this is in fact what occurs. The downward shift observed in the transition region during the flare is expected due to the increase in temperature and pressure locally in the flare, and hence the increase in the average value of the temperature and pressure. Further, we expect that the magnitude of the shift observed is proportional to the amount of stellar surface area covered by the flare.

Using ultraviolet line data from Dupree (1972), we can calculate a model of the solar chromosphere and transition region. These data include spectra of both the quiescent Sun and a solar active region. We may thus construct models of

TABLE 4A
MODEL FOR QUIESCENT STAR

log T	Pressure ($\times 10^{14}$)	Height ($\times 10^4$ km)	Height (scale heights)
3.60.....	3516.85	-16.85	-0.0828
3.70.....	3516.85	-16.85	-0.0828
3.80.....	2275.54	-16.46	-0.0809
3.90.....	247.91	-13.99	-0.0688
4.00.....	102.22	-12.75	-0.0626
4.10.....	21.66	-10.00	-0.0492
4.20.....	8.58	-7.94	-0.0390
4.30.....	2.53	-4.53	-0.0222
4.40.....	1.74	-3.21	-0.0158
4.50.....	1.60	-2.83	-0.0139
4.60.....	1.57	-2.71	-0.0133
4.70.....	1.56	-2.66	-0.0131
4.80.....	1.55	-2.62	-0.0129
4.90.....	1.55	-2.59	-0.0127
5.00.....	1.54	-2.55	-0.0125
5.10.....	1.53	-2.45	-0.0121
5.20.....	1.51	-2.12	-0.0104
5.30.....	1.40	0.00	0.0000
5.40.....	1.30	27.78	0.1365
5.50.....	0.67	332.50	1.6339

TABLE 4B
MODEL FOR FLARING STAR

log T	Pressure ($\times 10^{14}$)	Height ($\times 10^4$ km)	Height (scale heights)
3.60.....	1350.01	-16.66	-0.0819
3.70.....	496.17	-15.96	-0.0784
3.80.....	180.16	-15.06	-0.0740
3.90.....	69.77	-14.00	-0.0688
4.00.....	27.24	-12.68	-0.0623
4.10.....	11.75	-11.19	-0.0550
4.20.....	5.11	-9.34	-0.0459
4.30.....	2.74	-7.60	-0.0373
4.40.....	2.10	-6.65	-0.0327
4.50.....	1.90	-6.20	-0.0305
4.60.....	1.82	-5.97	-0.0294
4.70.....	1.78	-5.83	-0.0287
4.80.....	1.76	-5.72	-0.0281
4.90.....	1.74	-5.61	-0.0276
5.00.....	1.72	-5.45	-0.0268
5.10.....	1.70	-5.15	-0.0253
5.20.....	1.63	-4.31	-0.0212
5.30.....	1.40	0.00	0.0000
5.40.....	1.20	56.35	0.2769
5.50.....	0.48	479.20	2.3548

both the quiescent Sun and the active region, taking the active region to be representative of the surface of a hypothetical sun which is flaring over its entire surface. To compare these models to those of IM Peg, however, they must be scaled to correspond to the physical parameters observed on IM Peg. The similarity mentioned above between large solar flares and the stellar flare observed on IM Peg gives physical validity to this procedure, which will enable us to compare approximate solar and stellar models and so obtain an idea of the flare-filling factor.

The scaling process must take account of two differences between the Sun and IM Peg. First, the solar surface gravity must be scaled down to match that of IM Peg. Second, examination of equation (7) reveals that $dT/dh \sim 1/\text{EM}$; thus to obtain a scaled solar model comparable to an IM Peg model, the solar values of EM must be scaled to approximate those of

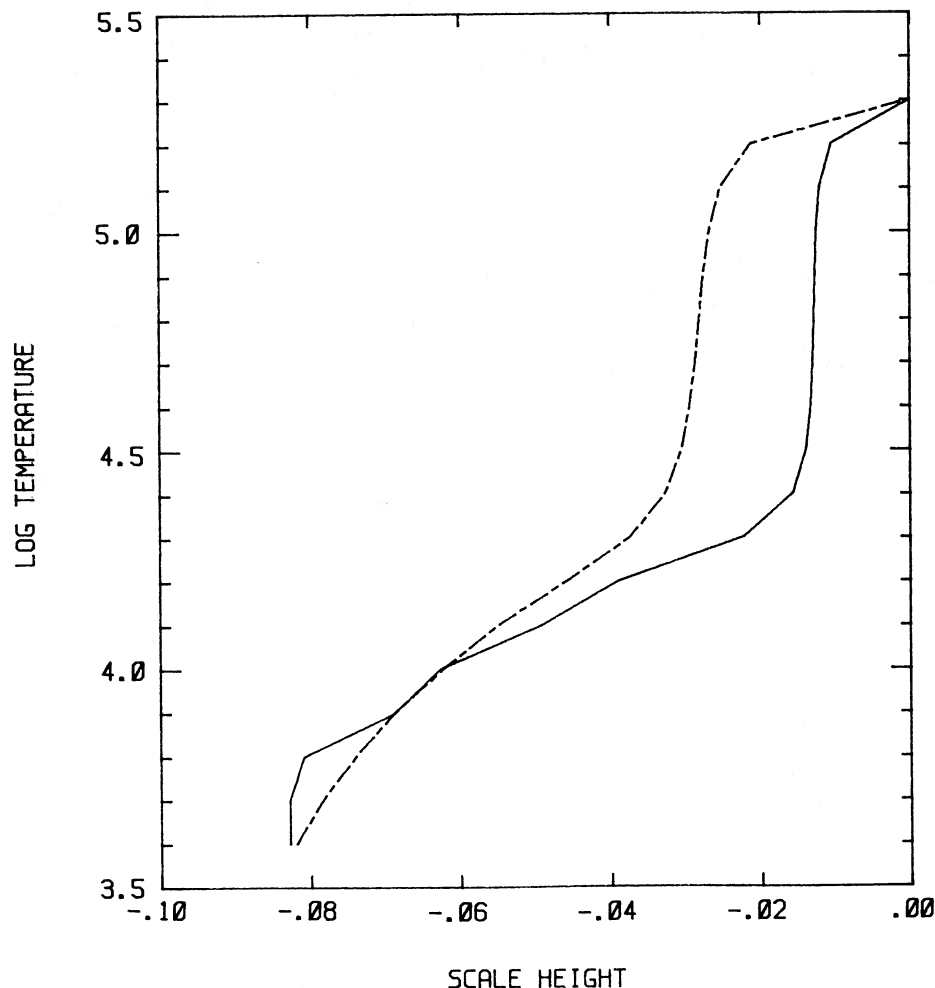


FIG. 3.—Variation of temperature with scale height for quiescent (*solid*) and flaring (*dashed*) IM Peg

IM Peg. We chose to scale based on the N v line, so

$$\text{EM}(\text{scaled}) = \frac{\text{EM}(\text{N v})_*}{\text{EM}(\text{N v})_{\odot}} \text{EM}(\text{solar}). \quad (15)$$

Carrying out these scaling procedures yields the scaled solar models shown in Figure 4. As above, the height scale is in units of transition region scale heights.

Comparison of the size, in scale heights, of the transition region shifts in the two sets of models leads to the conclusion that the IM Peg flare event covers about 30% of the surface area of the star at the altitude of the transition region. This is very large in comparison with a large solar flare, which might cover $\sim 0.1\%$ of the solar surface. It is important, however, to note that this flare size still represents a relatively small perturbation of the transition region pressure of the star; this justifies the assumption made earlier.

V. DISCUSSION

Figure 5 shows the variation of line enhancement ratios ($\text{Flux}[\text{flare}]/\text{Flux}[\text{quiescent}]$) as a function of $\log T$. It is apparent that significant differences exist between long-period ($P \gtrsim 14$ days) RS CVns and the shorter period RS CVns. The distribution of line enhancement ratios for long-period RS CVns is sharply peaked at a temperature coincident with the

transition region of the star, i.e., $\log T \sim 4.7\text{--}5.0$. This would seem to indicate that the greater part of the hot plasma responsible for radiation emission is at about this temperature. The two shorter period RS CVns, HR 1099 and UX Ari, behave differently; they display line enhancements which are monotonically increasing as a function of temperature over the temperature range available. Further, the enhancements observed are everywhere greater than those seen in the long-period stars. It is clear that the peak enhancement for these stars must occur at $\log T > 5.2$. Data from a flare star, Gliese 867A, and from a typical solar flare are plotted for comparison.

Swank *et al.* (1981) found that RS CVn atmospheres were characterized by coronae with (at least) two different temperature components. The low-temperature component has $\log T \sim 6.8$ while the high-temperature component has $\log T \sim 7.3\text{--}8.3$. X-ray variability is observed to be somewhat greater in the high-temperature component. Swank *et al.* also note that the longer period systems studied may require considerably less extensive high-temperature components to satisfy the requirements of the two-temperature corona model. This may occur because the longer period, more widely separated systems have less interaction between stars and may therefore produce less high-temperature plasma. Therefore, if RS CVn flares are caused by interstellar interactions such as those hypothesized by the flux tube theory of Simon, Linsky,

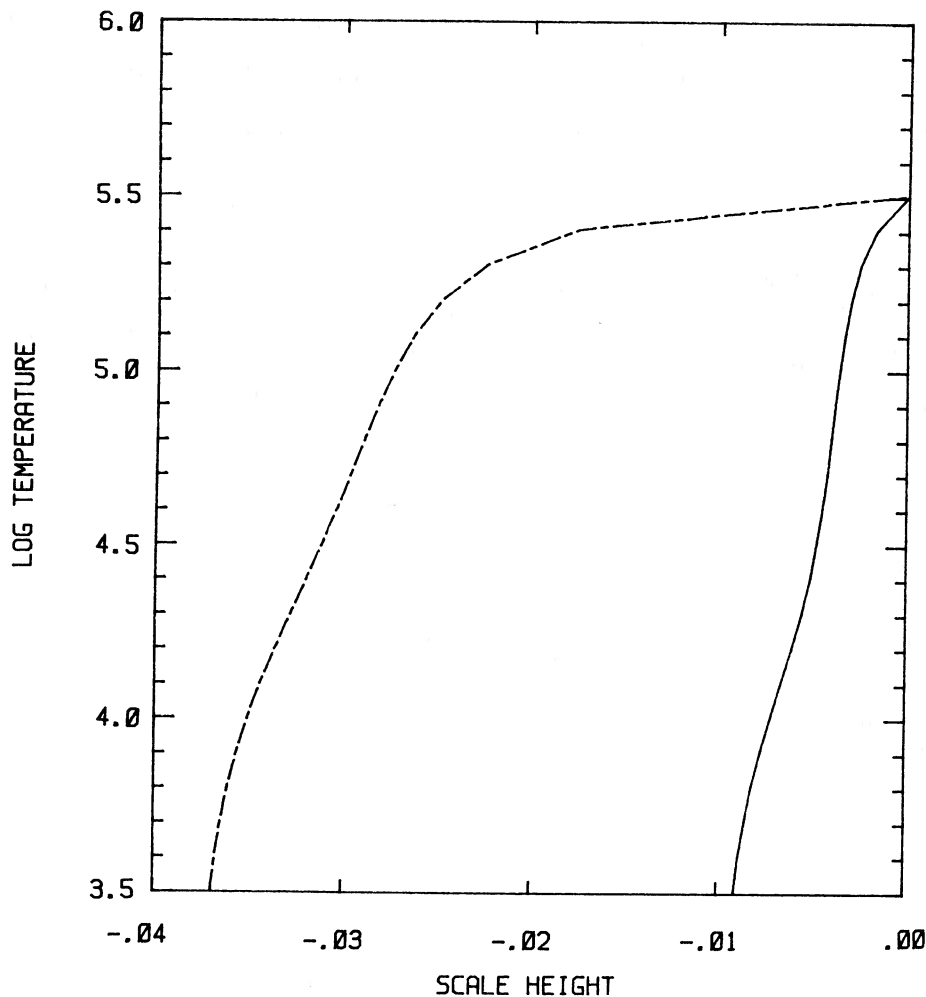


FIG. 4.—Temperature variation as a function of scale height for a scaled solar model. The flaring (*dashed*) model is calculated assuming that the entire solar surface is flaring.

and Schiffer (1980), we would expect flares on longer period systems such as IM Peg to occur at lower temperatures and lower altitudes, and to be smaller than those in shorter period systems such as HR 1099, since any such interaction which takes place must be lessened by distance.

A complete discussion of the errors inherent in emission measure analysis will not be attempted here; the reader is referred to Brown and Jordan (1981), Brown, Ferraz, and Jordan (1984), Withbroe (1975), or Jordan and Wilson (1971) for a more complete treatment. The greatest source of concern is the atomic data; for example, quoted errors for collision strengths are in some cases in excess of 50%. Furthermore, as Brown *et al.* (1984) have pointed out, some resonance lines, e.g., C II, Si IV, and C IV, are probably opacity broadened in β Draconis and there is no guarantee that this is not the case in IM Peg as well. However, the importance of many of these sources of error is minimized in this study as we are interested not in the absolute atmospheric model, but rather in the shift between two models with similar atomic parameters.

VI. CONCLUSIONS

We have measured the approximate area of a stellar flare using a method that does not depend on measurements of the stellar light curve and is not highly sensitive to model assump-

tions or errors. Furthermore, we note differences between flare events on RS CVn stars. The differences observed seem to correlate with the period of the system.

The flare event observed compares favorably with that observed by Baliunas, Guinan, and Dupree (1984) on λ And, which is also a long-period (~ 20.5 days) RS CVn star. Both flares showed that line enhancement as a function of temperature was sharply peaked at a temperature corresponding to the transition region, although the temperature of this peak was slightly cooler in λ And. In addition, both flares showed similar line enhancements and both had C IV more strongly enhanced than N V. This is in contrast to the situation observed during a flare on UX Ari, a short-period RS CVn star observed by Simon, Linsky, and Schiffer (1980). In this case, N V was enhanced more strongly than C IV; further, the sharp peak apparent in the two long-period variables was conspicuously absent, although the degree of line enhancement does tail off at lower temperatures. Even this gradual tailing off is absent in the spectra of a flare star such as Gliese 867A, which displays approximately uniform (and very low) enhancement across the entire temperature range (Butler *et al.* 1981). Differences in line enhancement as a function of temperature between short and long-period RS CVns can be qualitatively explained if flares are caused by interstellar interactions, such as those provided

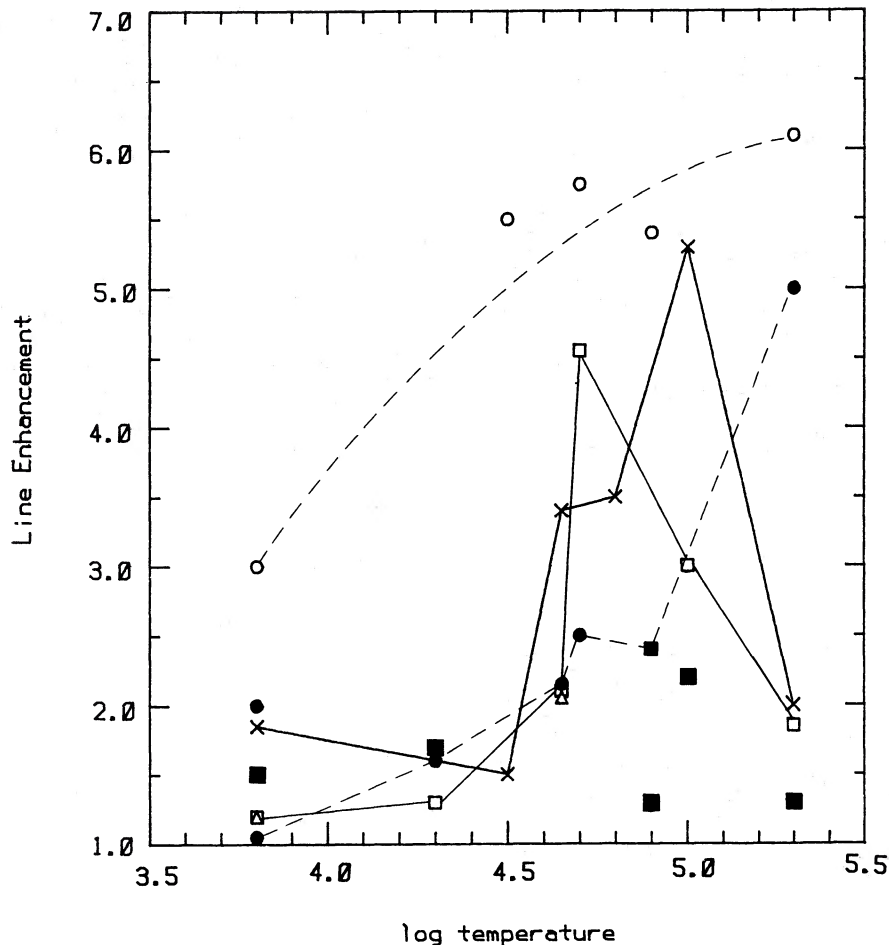


FIG. 5.—Line enhancement as a function of temperature for flares on selected objects. Solid lines are long-period RS CVns IM Peg (open squares) and λ And (crosses), while dashed lines are short-period RS CVns UX Ari (open circles) and HR 1099 (closed circles). A typical solar flare (triangles) and a flare on the flare star Gliese 867A (closed squares) are plotted for comparison.

by the flux tube theory, since such interactions would be weaker in long-period systems.

Higher resolution spectra would greatly enhance the reliability of this technique, by allowing a more accurate determination of the pressure at the top of the transition region through measurements of line strength ratios and line widths. In addition, such spectra would allow us to be sure that such

resonance lines as C IV are not significantly optically thick. X-ray observations would allow extension of the emission measure distribution upward of 2×10^5 K, perhaps to beyond 10^7 K. A determination of the area of the flare at such heights would perhaps be a good test of the flux tube model.

This work was supported by NASA grant NAG5-563.

REFERENCES

- Allen, C. W. 1973, *Astrophysical Quantities* (3rd ed.; London: Athlone).
 Baliunas, S. L., Guinan, E. F., and Dupree, A. K. 1984, *Ap. J.*, **282**, 733.
 Baliunas, S. L., Hartmann, L., Vaughan, A. H., Liller, W., and Dupree, A. K. 1981, *Ap. J.*, **246**, 473.
 Barnes, T. G., and Evans, D. S. 1976, *M.N.R.A.S.*, **174**, 489.
 Barnes, T. G., Evans, D. S., and Parsons, S. B. 1976, *M.N.R.A.S.*, **174**, 503.
 Brown, A., and Jordan, C. 1981, *M.N.R.A.S.*, **196**, 757.
 Brown, A., Jordan, C., Stencel, R. E., Linsky, J. L., and Ayres, T. R. 1984, *Ap. J.*, **283**, 731.
 Brown, A., Ferraz, M. C. de, and Jordan, C. 1984, *M.N.R.A.S.*, **207**, 831.
 Butler, C. J., Byrne, P. B., Andrews, A. D., and Doyle, J. G. 1981, *M.N.R.A.S.*, **197**, 815.
 Dupree, A. K. 1972, *Ap. J.*, **178**, 527.
 Eker, Z. 1984, University of Wisconsin preprint No. 212.
 Jordan, C. 1969, *M.N.R.A.S.*, **142**, 501.
 Jordan, C., and Wilson, R. 1971, in *Physics of the Solar Corona* (Dordrecht: Reidel), p. 219.
 Linsky, J. L. 1984, in *Cool Stars, Stellar Systems, and the Sun*, ed. S. L. Baliunas and L. Hartmann (Berlin: Springer), p. 244.
 Simon, T., Linsky, J. L., and Schiffer, F. H. III. 1980, *Ap. J.*, **239**, 911.
 Swank, J. H., White, N. E., Holt, S. S., and Becker, R. H. 1981, *Ap. J.*, **246**, 208.
 Weiler, E. J., et al. 1978, *Ap. J.*, **225**, 919.
 Withbroe, G. L. 1975, *Solar Phys.*, **45**, 301.

DEREK L. BUZASI, DAVID P. HUENEMOERDER, and LAWRENCE W. RAMSEY: Department of Astronomy, The Pennsylvania State University, University Park, PA 16802